FEBS Letters

FEBS PRESS science publishing by scientists

IN A NUTSHELL

Invisible but not inaccessible—Revealing transient oligomers formed by intrinsically disordered proteins with solution NMR and complementary methods

Martin D. Gelenter and Ad Bax

Laboratory of Chemical Physics, National Institute of Diabetes and Digestive and Kidney Diseases, National Institutes of Health, Bethesda, MD, USA

Correspondence
M. D. Gelenter and A. Bax, Laboratory of Chemical Physics, National Institute of Diabetes and Digestive and Kidney Diseases, National Institutes of Health, Bethesda, MD, 20892, USA
Tel: +1 301 594 8301 and +1 301 496 2848
E-mail: gelentermd@nih.gov; bax@nih.gov

(Received 20 July 2026, revised 9 August 2026, accepted 4 September 2026)

doi:10.1002/1873-3468.70474

Edited by Christian Griesinger

Intrinsically disordered proteins (IDPs) are often readily characterized as soluble monomers, whereas their biological and pathological roles frequently involve transient, heterogeneous, or sparsely populated oligomers. Such assemblies are often described as 'invisible' but invisibility is method-dependent: Oligomers that escape direct detection by one technique may remain accessible through indirect or complementary measurements. Solution NMR is uniquely positioned to exploit exchange between observable monomers and NMR-invisible oligomers, providing residue-specific information on populations, kinetics, and intermolecular contacts. Other methods report on mass, stoichiometry, dimensions, morphology, or site-specific distance distributions. Here, we discuss how integrating orthogonal measurements can overcome method-specific blind spots and yield a self-consistent model that simultaneously accounts for structure, populations, exchange kinetics, and morphology, something no single method can provide.

Keywords: amyloid; intrinsically disordered proteins; protein aggregation; solution NMR; spectroscopy; transient oligomers

Intrinsically disordered proteins (IDPs) are particularly well suited to solution nuclear magnetic resonance (NMR) spectroscopy [1–5]. Rapid segmental motions and conformational averaging produce sharp resonances, although limited ^{1}H chemical shift dispersion and rapid exchange of protons with water can cause substantial spectral overlap and signal loss, respectively [6–8]. Experiments that directly observe ^{13}C or ^{15}N nuclei can alleviate these limitations when conventional ^{1}H detection is unfavorable [3,6,8,9]. Local mobility weakens the correlation between molecular weight and linewidth, often keeping a large IDP observable when a globular protein of comparable mass would be difficult to study [1,10]. Yet the state that gives the cleanest spectrum is not necessarily the one that controls biological function or pathology [11–15]. Transient self-association has been observed for a diverse set of IDPs, producing oligomers that

Abbreviations
AFM, atomic force microscopy; ALS, amyotrophic lateral sclerosis; AUC, analytical ultracentrifugation; Aβ, amyloid-β; CEST, chemical exchange saturation transfer; CPMG, Carr–Purcell–Meiboom–Gill; cryo-EM, cryogenic electron microscopy; CTE, chronic traumatic encephalopathy; DEER, double electron–electron resonance; DEST, dark-state exchange saturation transfer; DLS, dynamic light scattering; eIF4B, eukaryotic translation initiation factor 4B; EPR, electron paramagnetic resonance; HSQC, heteronuclear single quantum coherence; IDP, intrinsically disordered protein; MS, mass spectrometry; NMR, nuclear magnetic resonance; NOE, nuclear Overhauser effect; nsFCS, nanosecond fluorescence correlation spectroscopy; PRE, paramagnetic relaxation enhancement; SAXS, small-angle X-ray scattering; SEC-MALS, size-exclusion chromatography coupled to multi-angle light scattering; smFRET, single-molecule Förster resonance energy transfer; ssNMR, solid-state NMR; TDP-43, TAR DNA-binding protein 43.

may be short-lived, sparsely populated [16], structurally heterogeneous [17], or in rapid exchange with monomer or other assemblies [18–22]. These properties can render transient oligomers difficult to characterize directly, even though such assemblies may regulate activity [14], nucleate further aggregation [16,23–25], or contribute directly to toxicity [17,26,27].

Here, a transient oligomer refers to a noncovalent assembly in reversible exchange with monomer or to a metastable intermediate along a self-association pathway (Fig. 1A). Transient oligomers can participate in functional assembly and precede condensate formation [14,28–32], but here we focus primarily on dispersed oligomers, particularly those associated with aggregation pathways. Mature fibrils and large phase-separated condensates fall outside the main scope of this Review, except where they clarify an aggregation pathway or when methods used to study them can also characterize transient oligomers [28–32].

This creates a recurring problem for structural biologists: The species of interest may only leave an indirect experimental signature. Oligomers may be too large or exchange too rapidly for conventional solution NMR [1,33], too heterogeneous for high-resolution solid-state NMR (ssNMR) or cryogenic electron microscopy (cryo-EM) reconstruction [34], too low in population for ensemble-averaged measurements, or too dynamic for methods that probe distances or morphology (Fig. 1B). The relevant question is therefore not whether transient oligomers are visible or invisible in an absolute sense, or which single technique is optimal, but what each method can 'see' and how complementary observables can be combined into a quantitative model of the oligomer ensemble.

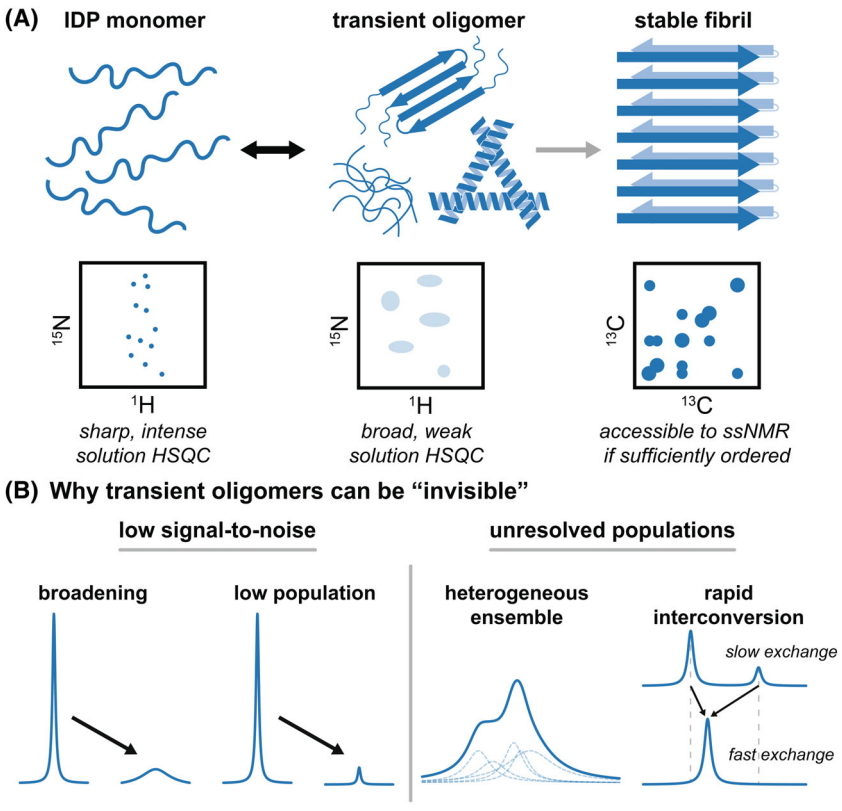

Fig. 1. Intrinsically disordered protein (IDP) assembly and why transient oligomers can be experimentally 'invisible'. (A) Disordered monomers often yield sharp, intense solution ^{1}H-^{15}N HSQC spectra, whereas transient oligomers may produce broad, weak, or undetectable signals because of slower tumbling, conformational heterogeneity, and chemical exchange. More persistent and sufficiently ordered fibrils can become accessible to ssNMR. Monomer–oligomer exchange is often reversible and couples all monomeric and oligomeric populations. Conversion to fibrils is typically much slower and effectively irreversible on the experimental time scale. The depicted oligomer structures illustrate possible disordered, β-sheet-rich, and α-helical assemblies and do not imply relative populations; transient oligomers are not necessarily on-pathway to fibrils. (B) Oligomer signals can be lost because line broadening or low population reduces signal-to-noise, or because heterogeneous populations prevent individual states from being resolved. Under rapid exchange, state-specific resonances coalesce into a single population-weighted resonance. These sources of invisibility are not mutually exclusive.

What makes an oligomer 'invisible'?

Here, 'invisible' does not mean absent, unimportant, or inaccessible to all measurements. It means that a species is not directly observed or uniquely resolved by a particular measurement. In solution NMR, the term is especially literal: Slow tumbling, conformational heterogeneity, and chemical exchange can accelerate transverse relaxation until the oligomer resonances broaden beyond detection (Fig. 1). The oligomer is therefore NMR-invisible, often referred to as a 'dark state', but exchange can leave measurable effects on visible monomer signals [18,33].

Other techniques can be 'blind' in different ways. Small or flexible oligomers may be visible as particles but inaccessible to high-resolution cryo-EM reconstruction [35]. Single-molecule Förster resonance energy transfer (smFRET) can detect low-population oligomers, but its structural information is limited to distances between selected dyes [36–38]. Native mass spectrometry can resolve distributions of oligomer stoichiometries, but the results can be biased by ionization and gas-phase transfer efficiencies [39]. Small-angle X-ray scattering (SAXS), analytical ultracentrifugation (AUC) [40], size-exclusion chromatography coupled to multi-angle light scattering (SEC-MALS) [41], and mass photometry report on overall dimensions, mass, or hydrodynamic behavior while leaving residue-level structure undetermined [42,43]. These various methods provide complementary rather than interchangeable views.

'Visible' should always be followed by a qualifier: visible to which measurement, over which timescale, and at what population? Signal broadening, low population, ensemble averaging, heterogeneity, short lifetime, and limited structural resolution are distinct experimental problems and call for different solutions (Fig. 1).

NMR sees 'dark' oligomer states through visible monomers

Solution NMR can probe transient oligomers without directly observing their resonances (Fig. 2A). When an NMR-visible monomer exchanges with an NMR-invisible oligomer, exchange can alter the peak positions, linewidths, or intensities of the monomer resonances in a residue-specific manner [33]. The simplest clue is often concentration-dependent peak broadening: resonances from affected residues broaden or weaken as self-association becomes more favorable [44]. Such changes can identify residues perturbed by self-association, but line broadening alone rarely defines a unique interface, exchange rate, or oligomer stoichiometry. Those quantities require an explicit kinetic model and, ideally, independent measurements. Exchange-based detection also has an important boundary condition: the dark oligomer must exchange with the observable state in a regime that measurably perturbs the monomer signal. The absence of concentration-dependent broadening or other exchange effects does not by itself exclude oligomerization.

Carr–Purcell–Meiboom–Gill (CPMG) and rotating-frame $R_{1\rho}$ relaxation dispersion experiments are especially sensitive to exchange on the microsecond-to-millisecond timescale [33,45]. Both detect a minor state indirectly by modulating how exchange affects transverse relaxation: CPMG varies the spacing, or frequency, of refocusing pulses, whereas $R_{1\rho}$ varies the strength or offset of a continuous spin-lock rf field. With an appropriate kinetic model, global fitting can estimate a minor-state population, exchange rate, and chemical-shift differences even when it has no resolved resonances [46–48]. Measurements at several protein concentrations or magnetic fields help separate otherwise correlated parameters. There is no universal optimal concentration because concentration itself shifts the oligomerization equilibrium. Concentration-dependent CPMG and $R_{1\rho}$ measurements of huntingtin-derived peptides revealed sparsely populated productive and nonproductive dimers and a tetrameric intermediate preceding fibril nucleation, with PRE and DEER data providing further structural information and validation [16].

Chemical exchange saturation transfer (CEST) and dark-state exchange saturation transfer (DEST) experiments detect exchange through saturation transfer [49]. In CEST, weak radiofrequency irradiation of a sufficiently long-lived minor state, often with a lifetime of several to ~100 milliseconds, transfers saturation to the major state, attenuating its resonance [50]. DEST instead exploits the broad saturation profile of a rapidly relaxing, high-molecular-weight species [51]. Applied to the Alzheimer's-associated peptide amyloid-β (Aβ), DEST identified residues in direct contact with protofibril surfaces and yielded monomer-protofibril exchange kinetics [18]. CEST and DEST are sometimes grouped together, but the distinction is useful for a broad audience: one resolves a minor-state frequency (CEST), whereas the other detects exchange with a resonance distribution too broad to observe directly (DEST).

Paramagnetic relaxation enhancement (PRE) introduces a spin label containing an unpaired electron, which can report on transient intermolecular contacts. Because the resulting relaxation enhancement depends

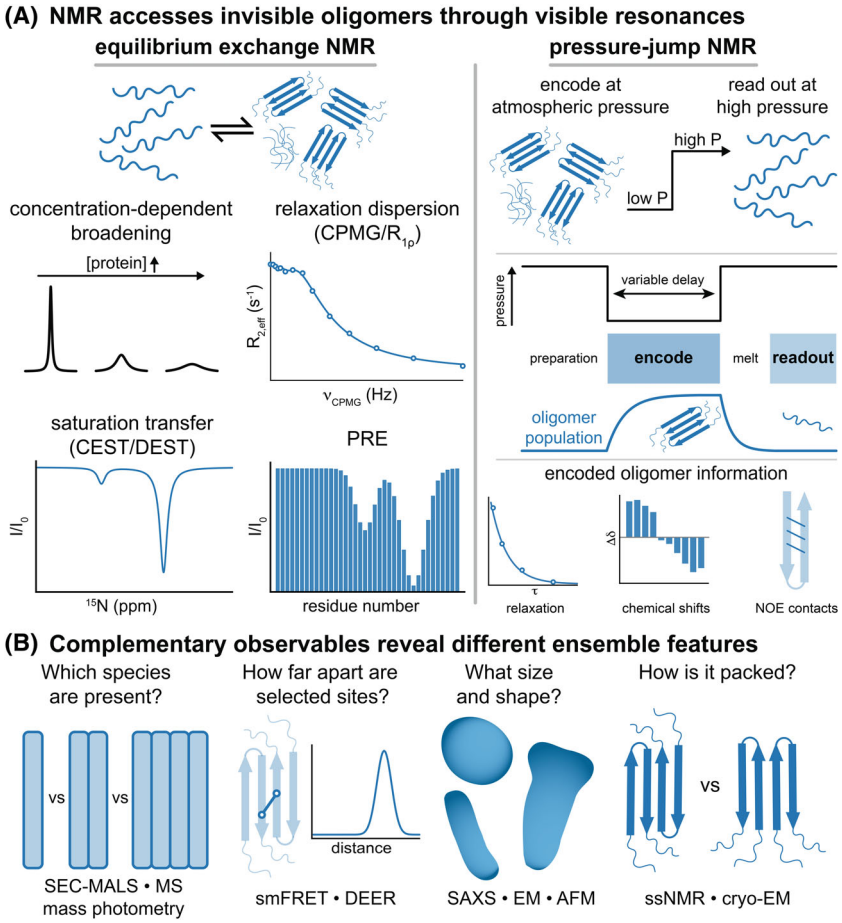

Fig. 2. Solution NMR and complementary measurements provide different views of transient oligomers. (A) At equilibrium, transient oligomers can be probed through concentration-dependent broadening of visible monomer resonances, CPMG or $R_{1\rho}$ relaxation dispersion, CEST or DEST saturation transfer, and intermolecular PRE. Non-equilibrium pressure-jump NMR instead encodes relaxation, chemical-shift, or NOE information while the oligomer is populated at atmospheric pressure and reads that information from sharp monomer resonances after a jump to high pressure. The melting period allows the oligomer population to dissociate sufficiently into dynamic monomer before the readout. Varying the intervals between pressure changes controls the time available for oligomerization or dissociation. The oligomer encoding period and readout can be positioned at defined time points relative to these pressure changes to follow the oligomer population and encoded observables over time. (B) Representative orthogonal measurements address complementary questions. SEC-MALS, native MS, and mass photometry report the masses or stoichiometries present; smFRET and DEER provide selected distance distributions; SAXS, EM, and AFM report overall dimensions or morphology; ssNMR and cryo-EM can reveal internal structure and packing when an oligomer is sufficiently ordered and persistent or can be enriched, trapped, or rapidly frozen.

steeply on the electron-nucleus distance, with an r^{-6} dependence, rare close contacts can dominate the measured relaxation enhancement [52]. Mixing isotopically labeled monomers with separately spin-labeled monomers allows intermolecular effects to be isolated. The measurement is highly sensitive to weak encounter complexes, but its interpretation depends on label position and mobility and generally describes a dynamic ensemble rather than a unique structure [53,54]. In the Parkinson's-associated IDP α-synuclein, intermolecular PREs detected weak N-to-C-terminal interchain contacts at neutral pH and stronger C-terminal contacts at low pH, illustrating how the transient contact ensemble can shift with solution conditions [55]. Intramolecular PREs have also mapped long-range contacts in unstructured α-synuclein that influence its aggregation propensity [56,57].

These equilibrium measurements cover overlapping parts of the association process, with their sensitivity depending on population, exchange rate, chemical-shift differences, and relaxation. Concentration-dependent NMR signal broadening maps where the observable state responds to association; relaxation dispersion and

saturation transfer constrain populations and exchange kinetics over different timescale windows; and intermolecular PREs report where chains make transient contacts. The most convincing mechanistic interpretation is one in which a single thermodynamic and kinetic model accounts simultaneously for all of these observables.

Whereas the preceding methods exploit equilibrium exchange, pressure-jump NMR actively perturbs the equilibrium population distribution [58–60]. For systems that oligomerize at atmospheric pressure and dissociate reversibly at high pressure [61,62], relaxation, chemical shift, or NOE information can be encoded while the oligomer is populated. A rapid jump to high pressure then shifts the equilibrium toward monomer, allowing the encoded information to be read from intense, sharp monomer resonances (Fig. 2A) [62]. Varying the delays within the pressure-jump sequence allows assembly or dissociation to be followed from milliseconds to minutes and, in principle, longer [58,60,63]. The method requires pressure to shift the population reversibly toward a detectable state, and the sample must tolerate repeated cycling without irreversible aggregation [64–66].

For $A\beta_{40}$, whose disease-implicated oligomers dissociate reversibly at high pressure, pressure-jump NMR enabled residue-specific measurements of oligomer relaxation [62] and long-range NOE contacts [66]. For amelotin, an intrinsically disordered enamel protein involved in mineralization, oligomer chemical shifts and long-range NOEs were measured using the same strategy [67]. For melittin, a non-amyloid peptide whose disordered monomer to helical tetramer equilibrium kinetics have been extensively studied, global fitting of pressure-jump kinetics with CPMG relaxation dispersion data identified a dimeric intermediate whose population never exceeded 1.6% but that was required for tetramer formation [63]. The value of the combination is more than the sum of its parts: the nonequilibrium pressure-jump data define the overall population trajectory, while equilibrium relaxation dispersion is particularly sensitive to the minor intermediate (Fig. 2A).

Complementary methods address what solution NMR misses

Solution NMR is strongest when residue-specific exchange, dynamics, or contacts are tied to mechanism. It is less direct for particle mass, stoichiometry, and morphology. Complementary methods are best chosen according to the missing observable (Fig. 2B).

Single-molecule fluorescence can detect rare oligomers and give information on their heterogeneity. Two-color coincidence reports whether differently labeled molecules co-assemble into the same oligomer [36]. smFRET adds one or more selected interdye distance restraints for additional structural or kinetic information [37,68–71]. In mixtures of $A\beta_{40}$ and $A\beta_{42}$, donor- and acceptor-labeled peptides revealed heterogeneous oligomers with extensive co-assembly of the two isoforms [38]. In the functional eIF4B intrinsically disordered domain, fluorescence correlation spectroscopy (FCS) and single-molecule fluorescence characterized oligomer growth and millisecond exchange, while nanosecond FCS (nsFCS) measured ~100–150 ns chain reconfiguration times; NMR, EM, and simulations linked these dynamics to oligomerization and subsequent condensate formation [72]. These approaches require fluorescent labels, which may perturb weak equilibria.

Electron paramagnetic resonance (EPR), specifically double electron–electron resonance (DEER), measures selected inter-spin-label distance distributions in frozen samples and is therefore not limited by slow molecular tumbling [73]. Inversion-modulated DEER can quantify relative monomer and oligomer populations [74], and helped establish transient huntingtin oligomers [16]. T_1-edited DEER further separates monomer- and dimer-specific distance distributions within mixed samples [75]. As with fluorescence, interpretation depends on the choice and flexibility of the spin-labeling sites. Freezing conditions must also be considered for DEER.

Native mass spectrometry and mass photometry address stoichiometry and particle mass from different directions. Native mass spectrometry can resolve oligomeric states, while ion mobility adds gas-phase collision cross sections. Applied to the diabetes-associated peptide amylin, this combination detected oligomers up to hexamers and distinguished their elongated conformations [76]. Ionization efficiency, gas-phase transfer, and dissociation of fragile assemblies can nevertheless bias apparent relative populations [39]. Mass photometry instead measures the scattering contrast of individual unlabeled particles as they land on a glass surface [43]. It yields a particle-mass distribution and has followed changes in low-order Alzheimer's-and-CTE-associated tau protein oligomers during aggregation [77], although its concentration range, lower mass limit, and surface dependence matter for weak equilibria.

AUC and SEC-MALS provide distinct solution-phase views of oligomerization. Sedimentation-velocity AUC reports distributions of sedimentation coefficients and supports quantitative models of reversible self-association [40]. SEC-MALS reports molar mass

across chromatographically separated peaks [41], but dilution and separation may perturb rapidly interconverting monomer-oligomer equilibria.

SAXS measures ensemble-averaged dimensions and low-resolution shape and can provide global restraints complementary to local NMR measurements [42,78–80], whereas dynamic light scattering (DLS) reports apparent hydrodynamic-size distributions but is disproportionately sensitive to larger particles [81]. Heterogeneous mixtures may therefore be difficult to deconvolve by either method. Electron microscopy (EM) and atomic force microscopy (AFM) provide direct views of morphology and sample heterogeneity, although grid preparation or surface adsorption can favor selected species [34].

Solid-state NMR and cryo-EM become especially informative when an oligomer is sufficiently persistent, enriched, trapped, or rapidly frozen (Fig. 2B). ssNMR has resolved a ~7% population of dynamic, largely disordered $A\beta_{40}$ oligomers that yielded only four sharp peaks in a solution ^{1}H-^{15}N HSQC spectrum [82], followed freeze-trapped $A\beta_{40}$ assemblies during early aggregation [83], and, together with super-resolution microscopy and simulations, characterized a toxic lipid-associated α-synuclein tetramer [84]. Cryo-EM has likewise revealed kinetically trapped α-synuclein oligomers [85] and, in combination with cryo-electron tomography and AFM, visualized Aβ oligomers, curvilinear protofibrils, and annular assemblies [86]. These methods can provide substantially greater structural detail than global size or mass measurements, but enrichment or trapping may bias the sampled ensemble and alter the populations present under native solution conditions.

At the persistent end of the assembly landscape, solid-state NMR has yielded high-resolution structures of brain-derived Aβ fibrils [87], monomorphic $A\beta_{42}$ fibrils [88,89], the nonhelical filament tau fibril [90], and pathogenic α-synuclein fibrils [91]. Cryo-EM has similarly determined the structures of patient-derived tau filaments [92] and both *in vitro* and brain-derived $A\beta_{42}$ fibrils [93,94]. These fibril structures do not directly describe transient oligomers; rather, they illustrate the structural detail that may become accessible when an oligomer is sufficiently persistent, homogeneous, or trapped.

The most useful combination is usually a small set of measurements that resolves a specific ambiguity (Table 1). Exchange rates do not define structure, selected distances do not establish stoichiometry, mass does not specify morphology, and a trapped high-resolution structure does not determine its native population or lifetime. Orthogonal measurements become decisive when they force the same model to account

Table 1. What different measurements contribute to an integrated model of transient oligomers.

Question	Representative measurements	Contribution to the integrated model	What remains unresolved
Which states are populated, how long-lived are they, and how rapidly do they interconvert?	CPMG, $R_{1\rho}$, CEST, DEST, pressure-jump NMR relaxation and kinetics	Residue-specific exchange rates, relative populations, lifetimes, chemical shift differences	Mass, stoichiometry, morphology, and detailed structure
What oligomeric species are present, and what are their masses?	SEC-MALS, AUC, mass photometry, native MS, and ion mobility	Molar mass and distributions of sedimentation coefficients, particle masses, and collision cross sections	Interfaces, structure, and method-dependent biases in apparent populations
Which residues or sites contact one another?	smFRET, DEER, PRE, pressure-jump NOE	Selected distance distributions and residue-specific contacts	Stoichiometry, global structure, population, lifetime, and ambiguity among models consistent with sparse restraints
What are the overall dimensions and shape?	EM, AFM, SAXS, DLS	Overall morphology, ensemble-averaged dimensions, hydrodynamic size	Residue-level structure, preparation bias, and quantitative populations of minor species
Where does an oligomer lie along the assembly pathway?	CPMG, $R_{1\rho}$, CEST, pressure-jump NMR kinetics	Constrains kinetic connectivity among populated states	Pathway assignments may not be unique; orthogonal measurements of mass, structure, or morphology are needed to identify the modeled states
What structural information can be determined for a sufficiently persistent or trapped state?	ssNMR, cryo-EM	Local structural restraints or three-dimensional reconstruction	Lifetime, exchange kinetics, and whether the selected state accurately represents the solution ensemble

for these distinct observables (Fig. 2). A recent study of the ALS-associated TDP-43 disordered C-terminal domain illustrates this principle: AUC constrained concentration-dependent multimerization, intermolecular NMR contacts localized the helical interface, and AlphaFold-Multimer combined with molecular dynamics simulations generated and tested compatible oligomer models [95–97].

What no method sees alone

Like disordered monomers [98–101], transient oligomers are best understood as ensembles rather than single static structures. For transient oligomers, that ensemble description must additionally include population, stoichiometry, lifetime, and exchange with monomer. A structural model without population or lifetime can overemphasize a rare species. A kinetic curve without residue-level information can miss the molecular event that controls assembly. Mass alone cannot distinguish whether an oligomer is compact or elongated, or identify the contacts that stabilize it. Indeed, morphologically similar oligomers can differ in internal packing and toxicity [26]. Likewise, a high-resolution structure of an enriched or trapped state may accurately describe one member of the ensemble while failing to represent the populations and exchange processes that dominate under native solution conditions [34].

An informative oligomer model should link population, lifetime, stoichiometry, residue-level contacts, dynamics, morphology, and position along the assembly pathway (Fig. 2, Table 1). Work on disordered monomers provides a useful precedent: combining complementary NMR observables with SAXS and smFRET has yielded quantitative ensemble descriptions that no single technique could provide [102–108]. For transient oligomers, orthogonal observables should similarly narrow the set of plausible models rather than be expected to produce one unique structure.

Meaningful integration also requires samples and conditions to be matched as closely as possible, with unavoidable differences included explicitly in the model. Concentration, buffer, temperature, labeling, surface interactions, and sample age may each shift a weak equilibrium, so nominally complementary experiments may probe different ensembles. Even under matched conditions, a model that reproduces all fitted data need not be unique because sparse, ensemble-averaged restraints may be satisfied by different combinations of populations and conformations [109,110]. Validation against independent observables withheld from fitting therefore provides a more rigorous test than agreement with the fitted data alone [109]. For transient oligomers, an additional test is whether the model predicts the effects of mutations and the response to changes in concentration, pressure, or temperature.

Transient oligomers are invisible only to particular measurements, not beyond the reach of structural biology. Their characterization therefore depends on integrating complementary observables into ensemble models that account simultaneously for structure, populations, exchange kinetics, and conformational dynamics. For IDPs, the sharp monomer spectrum often provides an experimental window through which otherwise invisible oligomer populations can be detected and characterized.

Acknowledgments

This research was supported by the Intramural Research Program of the National Institute of Diabetes and Digestive and Kidney Diseases (NIDDK) within the National Institutes of Health (NIH). The contributions of the NIH authors are considered Works of the United States Government. The findings and conclusions presented in this paper are those of the authors and do not necessarily reflect the views of the NIH or the U.S. Department of Health and Human Services. The authors used ChatGPT (OpenAI) to improve the readability of an author-written draft. The authors reviewed, edited, and rewrote all AI-suggested edits and take full responsibility for the content.

Author contributions

MDG conceptualized the review, generated figures, and wrote the initial draft. AB supervised and edited the manuscript. Both authors approved the final version.

References

1 Camacho-Zarco AR, Schnapka V, Guseva S, Abyzov A, Adamski W, Milles S, Jensen MR, Zidek L, Salvi N and Blackledge M (2022) NMR provides unique insight into the functional dynamics and interactions of intrinsically disordered proteins. *Chem Rev* **122**, 9331–9356.

2 van der Lee R, Buljan M, Lang B, Weatheritt RJ, Daughdrill GW, Dunker AK, Fuxreiter M, Gough J, Gsponer J, Jones DT *et al.* (2014) Classification of intrinsically disordered regions and proteins. *Chem Rev* **114**, 6589–6631.

3 Felli IC and Pierattelli R (2014) Novel methods based on ^{13}C detection to study intrinsically disordered proteins. *J Magn Reson* **241**, 115–125.
4 Konrat R (2014) NMR contributions to structural dynamics studies of intrinsically disordered proteins. *J Magn Reson* **241**, 74–85.
5 Eliezer D (2009) Biophysical characterization of intrinsically disordered proteins. *Curr Opin Struct Biol* **19**, 23–30.
6 Bermel W, Bertini I, Felli IC, Lee Y-M, Luchinat C and Pierattelli R (2006) Protonless NMR experiments for sequence-specific assignment of backbone nuclei in unfolded proteins. *J Am Chem Soc* **128**, 3918–3919.
7 Csizmok V, Felli IC, Tompa P, Banci L and Bertini I (2008) Structural and dynamic characterization of intrinsically disordered human Securin by NMR spectroscopy. *J Am Chem Soc* **130**, 16873–16879.
8 Felli IC and Pierattelli R (2022) ^{13}C direct detected NMR for challenging systems. *Chem Rev* **122**, 9468–9496.
9 Chhabra S, Fischer P, Takeuchi K, Dubey A, Ziarek JJ, Boeszoermenyi A, Mathieu D, Bermel W, Davey NE, Wagner G *et al.* (2018) ^{15}N detection harnesses the slow relaxation property of nitrogen: delivering enhanced resolution for intrinsically disordered proteins. *Proc Natl Acad Sci USA* **115**, E1710–E1719.
10 Kwan AH, Mobli M, Gooley PR, King GF and Mackay JP (2011) Macromolecular NMR spectroscopy for the non-spectroscopist. *FEBS J* **278**, 687–703.
11 Wright PE and Dyson HJ (2015) Intrinsically disordered proteins in cellular signalling and regulation. *Nat Rev Mol Cell Biol* **16**, 18–29.
12 Kriwacki RW, Hengst L, Tennant L, Reed SI and Wright PE (1996) Structural studies of p21Waf1/Cip1/Sdi1 in the free and Cdk2-bound state: conformational disorder mediates binding diversity. *Proc Natl Acad Sci USA* **93**, 11504–11509.
13 Haass C and Selkoe DJ (2007) Soluble protein oligomers in neurodegeneration: lessons from the Alzheimer's amyloid β-peptide. *Nat Rev Mol Cell Biol* **8**, 101–112.
14 Mas G, Burmann BM, Sharpe T, Claudi B, Bumann D and Hiller S (2020) Regulation of chaperone function by coupled folding and oligomerization. *Sci Adv* **6**, eabc5822.
15 Holehouse AS and Kragelund BB (2024) The molecular basis for cellular function of intrinsically disordered protein regions. *Nat Rev Mol Cell Biol* **25**, 187–211.
16 Kotler SA, Tugarinov V, Schmidt T, Ceccon A, Libich DS, Ghirlando R, Schwieters CD and Clore GM (2019) Probing initial transient oligomerization events facilitating huntingtin fibril nucleation at atomic resolution by relaxation-based NMR. *Proc Natl Acad Sci USA* **116**, 3562–3571.
17 Cremades N, Cohen SIA, Deas E, Abramov AY, Chen AY, Orte A, Sandal M, Clarke RW, Dunne P, Aprile FA *et al.* (2012) Direct observation of the interconversion of normal and toxic forms of α-synuclein. *Cell* **149**, 1048–1059.
18 Fawzi NL, Ying J, Ghirlando R, Torchia DA and Clore GM (2011) Atomic-resolution dynamics on the surface of amyloid-β protofibrils probed by solution NMR. *Nature* **480**, 268–272.
19 Cragnell C, Staby L, Lenton S, Kragelund BB and Skepö M (2019) Dynamical oligomerisation of histidine rich intrinsically disordered proteins is regulated through zinc-histidine interactions. *Biomolecules* **9**, 168.
20 Dear AJ, Michaels TCT, Meisl G, Klenerman D, Wu S, Perrett S, Linse S, Dobson CM and Knowles TPJ (2020) Kinetic diversity of amyloid oligomers. *Proc Natl Acad Sci USA* **117**, 12087–12094.
21 Michaels TCT, Šarić A, Curk S, Bernfur K, Arosio P, Meisl G, Dear AJ, Cohen SIA, Dobson CM, Vendruscolo M *et al.* (2020) Dynamics of oligomer populations formed during the aggregation of Alzheimer's Aβ42 peptide. *Nat Chem* **12**, 445–451.
22 Wei J, Meisl G, Dear AJ, Michaels TCT and Knowles TPJ (2025) Kinetics of amyloid oligomer formation. *Annu Rev Biophys* **54**, 185–207.
23 Karamanos TK, Jackson MP, Calabrese AN, Goodchild SC, Cawood EE, Thompson GS, Kalverda AP, Hewitt EW and Radford SE (2019) Structural mapping of oligomeric intermediates in an amyloid assembly pathway. *elife* **8**, e46574.
24 Cohen SIA, Linse S, Luheshi LM, Hellstrand E, White DA, Rajah L, Otzen DE, Vendruscolo M, Dobson CM and Knowles TPJ (2013) Proliferation of amyloid-β42 aggregates occurs through a secondary nucleation mechanism. *Proc Natl Acad Sci USA* **110**, 9758–9763.
25 Xu CK, Meisl G, Andrzejewska EA, Krainer G, Dear AJ, Castellana-Cruz M, Turi S, Edu IA, Vivacqua G, Jacquat RPB *et al.* (2024) α-Synuclein oligomers form by secondary nucleation. *Nat Commun* **15**, 7083.
26 Campioni S, Mannini B, Zampagni M, Pensalfini A, Parrini C, Evangelisti E, Relini A, Stefani M, Dobson CM, Cecchi C *et al.* (2010) A causative link between the structure of aberrant protein oligomers and their toxicity. *Nat Chem Biol* **6**, 140–147.
27 Fusco G, Chen SW, Williamson PTF, Cascella R, Perni M, Jarvis JA, Cecchi C, Vendruscolo M, Chiti F, Cremades N *et al.* (2017) Structural basis of membrane disruption and cellular toxicity by α-synuclein oligomers. *Science* **358**, 1440–1443.
28 Li P, Banjade S, Cheng H-C, Kim S, Chen B, Guo L, Llaguno M, Hollingsworth JV, King DS, Banani SF *et al.* (2012) Phase transitions in the assembly of multivalent signalling proteins. *Nature* **483**, 336–340.

29 Burke KA, Janke AM, Rhine CL and Fawzi NL (2015) Residue-by-residue view of in vitro FUS granules that bind the C-terminal domain of RNA polymerase II. *Mol Cell* **60**, 231–241.
30 Patel A, Lee HO, Jawerth L, Maharana S, Jahnel M, Hein MY, Stoynov S, Mahamid J, Saha S, Franzmann TM *et al.* (2015) A liquid-to-solid phase transition of the ALS protein FUS accelerated by disease mutation. *Cell* **162**, 1066–1077.
31 Murthy AC, Dignon GL, Kan Y, Zerze GH, Parekh SH, Mittal J and Fawzi NL (2019) Molecular interactions underlying liquid−liquid phase separation of the FUS low-complexity domain. *Nat Struct Mol Biol* **26**, 637–648.
32 Martin EW, Holehouse AS, Peran I, Farag M, Incicco JJ, Bremer A, Grace CR, Soranno A, Pappu RV and Mittag T (2020) Valence and patterning of aromatic residues determine the phase behavior of prion-like domains. *Science* **367**, 694–699.
33 Alderson TR and Kay LE (2020) Unveiling invisible protein states with NMR spectroscopy. *Curr Opin Struct Biol* **60**, 39–49.
34 Cawood EE, Karamanos TK, Wilson AJ and Radford SE (2021) Visualizing and trapping transient oligomers in amyloid assembly pathways. *Biophys Chem* **268**, 106505.
35 Toader B, Sigworth FJ and Lederman RR (2023) Methods for cryo-EM single particle reconstruction of macromolecules having continuous heterogeneity. *J Mol Biol* **435**, 168020.
36 Orte A, Birkett NR, Clarke RW, Devlin GL, Dobson CM and Klenerman D (2008) Direct characterization of amyloidogenic oligomers by single-molecule fluorescence. *Proc Natl Acad Sci USA* **105**, 14424–14429.
37 Schuler B, Soranno A, Hofmann H and Nettels D (2016) Single-molecule FRET spectroscopy and the polymer physics of unfolded and intrinsically disordered proteins. *Annu Rev Biophys* **45**, 207–231.
38 Meng F, Kim J-Y, Louis JM and Chung HS (2024) Single-molecule characterization of heterogeneous oligomer formation during co-aggregation of 40- and 42-residue amyloid-β. *J Am Chem Soc* **146**, 24426–24439.
39 Heck AJR (2008) Native mass spectrometry: a bridge between interactomics and structural biology. *Nat Methods* **5**, 927–933.
40 Howlett GJ, Minton AP and Rivas G (2006) Analytical ultracentrifugation for the study of protein association and assembly. *Curr Opin Chem Biol* **10**, 430–436.
41 Wen J, Arakawa T and Philo JS (1996) Size-exclusion chromatography with on-line light-scattering, absorbance, and refractive index detectors for studying proteins and their interactions. *Anal Biochem* **240**, 155–166.
42 Bernadó P and Svergun DI (2012) Structural analysis of intrinsically disordered proteins by small-angle X-ray scattering. *Mol BioSyst* **8**, 151–167.
43 Soltermann F, Foley EDB, Pagnoni V, Galpin M, Benesch JLP, Kukura P and Struwe WB (2020) Quantifying protein–protein interactions by molecular counting with mass photometry. *Angew Chem Int Ed* **59**, 10774–10779.
44 Fawzi NL, Ying J, Torchia DA and Clore GM (2010) Kinetics of amyloid β monomer-to-oligomer exchange by NMR relaxation. *J Am Chem Soc* **132**, 9948–9951.
45 Palmer AG (2014) Chemical exchange in biomacromolecules: past, present, and future. *J Magn Reson* **241**, 3–17.
46 Sugase K, Dyson HJ and Wright PE (2007) Mechanism of coupled folding and binding of an intrinsically disordered protein. *Nature* **447**, 1021–1025.
47 Schneider R, Maurin D, Communie G, Kragelj J, Hansen DF, Ruigrok RWH, Jensen MR and Blackledge M (2015) Visualizing the molecular recognition trajectory of an intrinsically disordered protein using multinuclear relaxation dispersion NMR. *J Am Chem Soc* **137**, 1220–1229.
48 Delaforge E, Kragelj J, Tengo L, Palencia A, Milles S, Bouvignies G, Salvi N, Blackledge M and Jensen MR (2018) Deciphering the dynamic interaction profile of an intrinsically disordered protein by NMR exchange spectroscopy. *J Am Chem Soc* **140**, 1148–1158.
49 Tugarinov V, Ceccon A and Clore GM (2022) NMR methods for exploring 'dark' states in ligand binding and protein-protein interactions. *Prog Nucl Magn Reson Spectrosc* **128**, 1–24.
50 Vallurupalli P, Bouvignies G and Kay LE (2012) Studying 'invisible' excited protein states in slow exchange with a major state conformation. *J Am Chem Soc* **134**, 8148–8161.
51 Fawzi NL, Ying J, Torchia DA and Clore GM (2012) Probing exchange kinetics and atomic resolution dynamics in high-molecular-weight complexes using dark-state exchange saturation transfer NMR spectroscopy. *Nat Protoc* **7**, 1523–1533.
52 Clore GM and Iwahara J (2009) Theory, practice, and applications of paramagnetic relaxation enhancement for the characterization of transient low-population states of biological macromolecules and their complexes. *Chem Rev* **109**, 4108–4139.
53 Tang C, Iwahara J and Clore GM (2006) Visualization of transient encounter complexes in protein–protein association. *Nature* **444**, 383–386.
54 Mateos B, Konrat R, Pierattelli R and Felli IC (2019) NMR characterization of long-range contacts in intrinsically disordered proteins from paramagnetic relaxation enhancement in 13C direct-detection experiments. *Chembiochem* **20**, 335–339.

55 Wu K-P and Baum J (2010) Detection of transient interchain interactions in the intrinsically disordered protein α-synuclein by NMR paramagnetic relaxation enhancement. *J Am Chem Soc* **132**, 5546–5547.

56 Bertoncini CW, Jung Y-S, Fernandez CO, Hoyer W, Griesinger C, Jovin TM and Zweckstetter M (2005) Release of long-range tertiary interactions potentiates aggregation of natively unstructured α-synuclein. *Proc Natl Acad Sci USA* **102**, 1430–1435.

57 Dedmon MM, Lindorff-Larsen K, Christodoulou J, Vendruscolo M and Dobson CM (2005) Mapping long-range interactions in α-synuclein using spin-label NMR and ensemble molecular dynamics simulations. *J Am Chem Soc* **127**, 476–477.

58 Kremer W, Arnold M, Munte CE, Hartl R, Erlach MB, Koehler J, Meier A and Kalbitzer HR (2011) Pulsed pressure perturbations, an extra dimension in NMR spectroscopy of proteins. *J Am Chem Soc* **133**, 13646–13651.

59 Roche J, Dellarole M, Caro JA, Norberto DR, Garcia AE, Garcia-Moreno B, Roumestand C and Royer CA (2013) Effect of internal cavities on folding rates and routes revealed by real-time pressure-jump NMR spectroscopy. *J Am Chem Soc* **135**, 14610–14618.

60 Charlier C, Alderson TR, Courtney JM, Ying J, Anfinrud P and Bax A (2018) Study of protein folding under native conditions by rapidly switching the hydrostatic pressure inside an NMR sample cell. *Proc Natl Acad Sci USA* **115**, E4169–E4178.

61 Sasaki K, Gaikwad J, Hashiguchi S, Kubota T, Sugimura K, Kremer W, Kalbitzer HR and Akasaka K (2008) Reversible monomer-oligomer transition in human prion protein. *Prion* **2**, 118–122.

62 Barnes CA, Robertson AJ, Louis JM, Anfinrud P and Bax A (2019) Observation of β-amyloid peptide oligomerization by pressure-jump NMR spectroscopy. *J Am Chem Soc* **141**, 13762–13766.

63 Gelenter MD, Yau W-M, Anfinrud PA and Bax A (2024) From milliseconds to minutes: melittin self-assembly from concerted non-equilibrium pressure-jump and equilibrium relaxation nuclear magnetic resonance. *J Phys Chem Lett* **15**, 1930–1935.

64 Roche J and Royer CA (2018) Lessons from pressure denaturation of proteins. *J R Soc Interface* **15**, 20180244.

65 Roche J, Royer CA and Roumestand C (2019) Chapter eleven - exploring protein conformational landscapes using high-pressure NMR. In Biological NMR Part A (Wand AJ, ed.), pp. 293–320. Academic Press.

66 Gelenter MD, Li T, Anfinrud P and Bax A (2026) Opportunities and challenges in the use of pressure-jump NMR to study Aβ and protein oligomerization. *Methods Enzymol* **729**, 179–230.

67 Chiliveri SC, Shen Y, Baber JL, Ying J, Sagar V, Wistow G, Anfinrud P and Bax A (2023) Experimental NOE, chemical shift, and proline isomerization data provide detailed insights into amelotin oligomerization. *J Am Chem Soc* **145**, 18063–18074.

68 Trexler AJ and Rhoades E (2010) Single molecule characterization of α-synuclein in aggregation-prone states. *Biophys J* **99**, 3048–3055.

69 Nath A, Sammalkorpi M, DeWitt DC, Trexler AJ, Elbaum-Garfinkle S, O'Hern CS and Rhoades E (2012) The conformational ensembles of α-synuclein and tau: combining single-molecule FRET and simulations. *Biophys J* **103**, 1940–1949.

70 Hofmann H, Soranno A, Borgia A, Gast K, Nettels D and Schuler B (2012) Polymer scaling laws of unfolded and intrinsically disordered proteins quantified with single-molecule spectroscopy. *Proc Natl Acad Sci USA* **109**, 16155–16160.

71 Ferreon ACM, Ferreon JC, Wright PE and Deniz AA (2013) Modulation of allostery by protein intrinsic disorder. *Nature* **498**, 390–394.

72 Swain BC, Sarkis P, Ung V, Rousseau S, Fernandez L, Meltonyan A, Aho VE, Mercadante D, Mackereth CD and Aznauryan M (2024) Disordered regions of human eIF4B orchestrate a dynamic self-association landscape. *Nat Commun* **15**, 8766.

73 Jeschke G (2012) DEER distance measurements on proteins. *Annu Rev Phys Chem* **63**, 419–446.

74 Schmidt T, Ghirlando R, Baber J and Clore GM (2016) Quantitative resolution of monomer-dimer populations by inversion modulated DEER EPR spectroscopy. *ChemPhysChem* **17**, 2987–2991.

75 Schmidt T, Kubatova N and Clore GM (2024) Deconvoluting monomer- and dimer-specific distance distributions between spin labels in a monomer/dimer mixture using T_1-edited DEER EPR spectroscopy. *J Am Chem Soc* **146**, 17964–17973.

76 Young LM, Cao P, Raleigh DP, Ashcroft AE and Radford SE (2014) Ion mobility spectrometry–mass spectrometry defines the oligomeric intermediates in amylin amyloid formation and the mode of action of inhibitors. *J Am Chem Soc* **136**, 660–670.

77 Paul SS, Lyons A, Kirchner R and Woodside MT (2022) Quantifying oligomer populations in real time during protein aggregation using single-molecule mass photometry. *ACS Nano* **16**, 16462–16470.

78 Grishaev A, Wu J, Trewhella J and Bax A (2005) Refinement of multidomain protein structures by combination of solution small-angle X-ray scattering and NMR data. *J Am Chem Soc* **127**, 16621–16628.

79 Grishaev A, Tugarinov V, Kay LE, Trewhella J and Bax A (2008) Refined solution structure of the 82-kDa enzyme malate synthase G from joint NMR and synchrotron SAXS restraints. *J Biomol NMR* **40**, 95–106.

80 Giehm L, Svergun DI, Otzen DE and Vestergaard B (2011) Low-resolution structure of a vesicle disrupting alpha-synuclein oligomer that accumulates during fibrillation. *Proc Natl Acad Sci USA* **108**, 3246–3251.
81 Stetefeld J, McKenna SA and Patel TR (2016) Dynamic light scattering: a practical guide and applications in biomedical sciences. *Biophys Rev* **8**, 409–427.
82 Kotler SA, Brender JR, Vivekanandan S, Suzuki Y, Yamamoto K, Monette M, Krishnamoorthy J, Walsh P, Cauble M, Banaszak Holl MM *et al.* (2015) High-resolution NMR characterization of low abundance oligomers of amyloid-β without purification. *Sci Rep* **5**, 11811.
83 Jeon J, Yau W-M and Tycko R (2023) Early events in amyloid-β self-assembly probed by time-resolved solid state NMR and light scattering. *Nat Commun* **14**, 2964.
84 Sant V, Matthes D, Mazal H, Antonschmidt L, Wieser F, Movellan KT, Xue K, Nimerovsky E, Stampolaki M, Nathan M *et al.* (2025) Lipidic folding pathway of α-synuclein via a toxic oligomer. *Nat Commun* **16**, 760.
85 Chen SW, Drakulic S, Deas E, Ouberai M, Aprile FA, Arranz R, Ness S, Roodveldt C, Guilliams T, De-Genst EJ *et al.* (2015) Structural characterization of toxic oligomers that are kinetically trapped during α-synuclein fibril formation. *Proc Natl Acad Sci USA* **112**, E1994–E2003.
86 Liang R, Khursheed A, Tahirbegi B, Torres-Flores AP, Qi S, Tian Y, Zhang H, Szwedziak P, Volkov VA, Darbari VC *et al.* (2025) Amyloid-β oligomers, curvilinear and annular assemblies, imaged by cryo-ET, cryo-EM, and AFM. *Sci Adv* **11**, eadx9030.
87 Lu J-X, Qiang W, Yau W-M, Schwieters CD, Meredith SC and Tycko R (2013) Molecular structure of β-amyloid fibrils in Alzheimer's disease brain tissue. *Cell* **154**, 1257–1268.
88 Colvin MT, Silvers R, Ni QZ, Can TV, Sergeyev I, Rosay M, Donovan KJ, Michael B, Wall J, Linse S *et al.* (2016) Atomic resolution structure of monomorphic Aβ42 amyloid fibrils. *J Am Chem Soc* **138**, 9663–9674.
89 Wälti MA, Ravotti F, Arai H, Glabe CG, Wall JS, Böckmann A, Güntert P, Meier BH and Riek R (2016) Atomic-resolution structure of a disease-relevant Aβ(1–42) amyloid fibril. *Proc Natl Acad Sci USA* **113**, E4976–E4984.
90 Duan P, Dregni AJ, Mammeri NE and Hong M (2023) Structure of the nonhelical filament of the Alzheimer's disease tau core. *Proc Natl Acad Sci USA* **120**, e2310067120.
91 Tuttle MD, Comellas G, Nieuwkoop AJ, Covell DJ, Berthold DA, Kloepper KD, Courtney JM, Kim JK, Barclay AM, Kendall A *et al.* (2016) Solid-state NMR structure of a pathogenic fibril of full-length human α-synuclein. *Nat Struct Mol Biol* **23**, 409–415.
92 Fitzpatrick AWP, Falcon B, He S, Murzin AG, Murshudov G, Garringer HJ, Crowther RA, Ghetti B, Goedert M and Scheres SHW (2017) Cryo-EM structures of tau filaments from Alzheimer's disease. *Nature* **547**, 185–190.
93 Gremer L, Schölzel D, Schenk C, Reinartz E, Labahn J, Ravelli RBG, Tusche M, Lopez-Iglesias C, Hoyer W, Heise H *et al.* (2017) Fibril structure of amyloid-β (1–42) by cryo–electron microscopy. *Science* **358**, 116–119.
94 Yang Y, Arseni D, Zhang W, Huang M, Lövestam S, Schweighauser M, Kotecha A, Murzin AG, Peak-Chew SY, Macdonald J *et al.* (2022) Cryo-EM structures of amyloid-β 42 filaments from human brains. *Science* **375**, 167–172.
95 Jumper J, Evans R, Pritzel A, Green T, Figurnov M, Ronneberger O, Tunyasuvunakool K, Bates R, Žídek A, Potapenko A *et al.* (2021) Highly accurate protein structure prediction with AlphaFold. *Nature* **596**, 583–589.
96 Evans R, O'Neill M, Pritzel A, Antropova N, Senior A, Green T, Žídek A, Bates R, Blackwell S, Yim J *et al.* (2022) Protein complex prediction with AlphaFold-Multimer. *bioRxiv* 2021.10.04.463034. doi: 10.1101/2021.10.04.463034
97 Rizuan A, Shenoy J, Mohanty P, dos Passos PM, Mercado Ortiz JF, Bai L, Viswanathan R, Zaborowsky J, Wang S-H, Johnson V *et al.* (2025) Structural details of helix-mediated multimerization of the conserved region of TDP-43 C-terminal domain. *Nat Commun* **16**, 10528.
98 Uversky VN, Gillespie JR and Fink AL (2000) Why are 'natively unfolded' proteins unstructured under physiologic conditions. *Proteins Struct Funct Genet* **41**, 415–427.
99 Tompa P (2002) Intrinsically unstructured proteins. *Trends Biochem Sci* **27**, 527–533.
100 Forman-Kay JD and Mittag T (2013) From sequence and forces to structure, function, and evolution of intrinsically disordered proteins. *Structure* **21**, 1492–1499.
101 Lindorff-Larsen K and Kragelund BB (2021) On the potential of machine learning to examine the relationship between sequence, structure, dynamics and function of intrinsically disordered proteins. *J Mol Biol* **433**, 167196.
102 Jensen MR, Markwick PRL, Meier S, Griesinger C, Zweckstetter M, Grzesiek S, Bernadó P and Blackledge M (2009) Quantitative determination of the conformational properties of partially folded and intrinsically disordered proteins using NMR dipolar couplings. *Structure* **17**, 1169–1185.

103 Mantsyzov AB, Maltsev AS, Ying J, Shen Y, Hummer G and Bax A (2014) A maximum entropy approach to the study of residue-specific backbone angle distributions in α-synuclein, an intrinsically disordered protein. *Protein Sci* **23**, 1275–1290.
104 Schwalbe M, Ozenne V, Bibow S, Jaremko M, Jaremko L, Gajda M, Jensen MR, Biernat J, Becker S, Mandelkow E *et al*. (2014) Predictive atomic resolution descriptions of intrinsically disordered hTau40 and α-synuclein in solution from NMR and small angle scattering. *Structure* **22**, 238–249.
105 Fuertes G, Banterle N, Ruff KM, Chowdhury A, Mercadante D, Koehler C, Kachala M, Estrada Girona G, Milles S, Mishra A *et al*. (2017) Decoupling of size and shape fluctuations in heteropolymeric sequences reconciles discrepancies in SAXS vs. FRET measurements. *Proc Natl Acad Sci USA* **114**, E6342–E6351.
106 Gomes G-NW, Krzeminski M, Namini A, Martin EW, Mittag T, Head-Gordon T, Forman-Kay JD and Gradinaru CC (2020) Conformational ensembles of an intrinsically disordered protein consistent with NMR, SAXS, and single-molecule FRET. *J Am Chem Soc* **142**, 15697–15710.
107 Schiavina M, Salladini E, Murrali MG, Tria G, Felli IC, Pierattelli R and Longhi S (2020) Ensemble description of the intrinsically disordered N-terminal domain of the Nipah virus P/V protein from combined NMR and SAXS. *Sci Rep* **10**, 19574.
108 Naudi-Fabra S, Tengo M, Jensen MR, Blackledge M and Milles S (2021) Quantitative description of intrinsically disordered proteins using single-molecule FRET, NMR, and SAXS. *J Am Chem Soc* **143**, 20109–20121.
109 Bonomi M, Heller GT, Camilloni C and Vendruscolo M (2017) Principles of protein structural ensemble determination. *Curr Opin Struct Biol* **42**, 106–116.
110 Berlin K, Castañeda CA, Schneidman-Duhovny D, Sali A, Nava-Tudela A and Fushman D (2013) Recovering a representative conformational ensemble from underdetermined macromolecular structural data. *J Am Chem Soc* **135**, 16595–16609.